PCCP

PAPER

View Article Online
View Journal | View Issue

Cite this: *Phys. Chem. Chem. Phys.*, 2017, **19**, 28175

The promotion effects of thionation and isomerization on charge carrier mobility in naphthalene diimide crystals

Daoyuan Zheng,[ac] Mingxing Zhang[ab] and Guangjiu Zhao *[ab]

Received 6th June 2017,
Accepted 20th September 2017

DOI: 10.1039/c7cp03787b

rsc.li/pccp

Herein, the promotion effects of thionation and isomerization on the carrier mobility properties of naphthalene diimide and thionated naphthalene diimide crystals were investigated in detail based on the Marcus–Hush theory and quantum-chemical calculations. The thionation of NDIs will improve the charge mobility of both electrons and holes, which is similar to the thionation of PDIs. The compound P only behaves as an n-type organic semiconductor (OSC), whereas the three other thionation structures have higher mobility values and can behave as p-type OSCs. For the *cis*/*trans* isomers of the two double-thionation structures, *trans*-S2 has a larger hole and electron carrier mobility than *cis*-S2; this is consistent with the experimental results obtained for *cis*–*trans*-isomers. A potential strategy for the development of high performance ambipolar OSCs is the substitution of O atoms by S atoms. These results will provide a guide for the design and optimization of OSCs *via* analysis of the relationship between carrier mobility and molecular crystal structures.

1. Introduction

Organic semiconductors (OSCs) have attracted significant attention in the research and applications of organic electronics such as organic light-emitting diodes (OLEDs), organic field-effect transistors (OFETs), and organic solar cells.[1–5] Compared with inorganic semiconductors (ISCs), OSCs have the merit of abundant structures and their properties can be easily modified by different substituents.[6–8] These characteristics not only extend their applications, but also benefit the fabrication of new OSCs. As one of the most important parameters, charge carrier mobility is frequently used to evaluate the properties of organic materials. Recently, the best performance of n-type OSC was shown by C_{60}, which exhibited an electron mobility of only 11 $cm^2\ V^{-1}\ s^{-1}$,[9] whereas the highest hole mobility values of 2,7-dioctyl[1]benzothieno[3,2-*b*][1]benzothiophene (C_8-BTBT) and rubrene reached 43 and 40 $cm^2\ V^{-1}\ s^{-1}$, respectively.[10,11] Additionally, n-type OSCs not only exhibit lower mobility, but also show less species and intrinsic instability as compared to the p-type OSCs.[8,12]

Naphthalene diimides (NDIs) and perylene diimides (PDI) are the most important n-type OSCs, which have been first observed in 1996 by Laquindanum and Horowitz.[13,14] The highest electron mobility in NDIs is 6.2 $cm^2\ V^{-1}\ s^{-1}$ with cyclohexyl as the *N*-substituted group,[15] whereas some other OSCs devices with NDIs as their core also show an electron mobility of *ca.* 1 $cm^2\ V^{-1}\ s^{-1}$.[15–18] The main methods for the design of high performance OSCs in NDIs and PDIs involve changing the groups at the nitrogen positions or halogen substitution in the naphthalene/perylene cores. Recently, NDIs have been proven as p-type or ambipolar OSCs by fusing tetrathiafulvalene into the NDI frameworks, and they possess a hole mobility as high as 0.31 $cm^2\ V^{-1}\ s^{-1}$.[19] Another strategy for designing OSCs with higher hole mobility is the replacement of O atoms by S.[20–22] Recently, a series of thionated NDIs were synthesized and characterized by Seferos *et al.*, and they measured the electron mobility of thin film transistors.[23] They found that the electron mobility of the thionated derivatives were three orders of magnitude higher than those of the non-thionated parent analogue, with the highest mobility reaching 0.075 $cm^2\ V^{-1}\ s^{-1}$ for *cis*-S2. Another significant result is that the electron mobility does not increase with the increasing number of sulfur atoms; this is different from the case of thionated PDIs. In the experiment for thionated PDIs, they found a strong positive correlation between electron mobility and degree of thionation.[22] We were interested in whether thionated NDIs could be used as ambipolar OSCs and the effects of thionation and isomerization on carrier mobility.

[a] *State Key Laboratory of Molecular Reaction Dynamics, Dalian Institute of Chemical Physics, Chinese Academy of Sciences, Dalian 116023, China. E-mail: gjzhao@dicp.ac.cn; Fax: +86-411-84675584; Tel: +86-411-84379692*
[b] *Tianjin Key Laboratory of Molecular Optoelectronic Science, Institute of Chemistry, Department of Chemistry, School of Science, Tianjin University, Tianjin 300072, China*
[c] *University of the Chinese Academy of Sciences, Chinese Academy of Sciences, Beijing 100049, China*

For interpreting the mechanisms of carrier mobility in OSCs, several theories have been proposed such as the hopping, band, and polaron models.[24] The hopping model has been proven to be reliable to investigate the quantitative structure–activity relationships of transport properties in a series of organic semiconductors such as acenes, oligothiophenes, and NDIs.[25–30] Herein, based on the quantum-chemical calculations and the Marcus–Hush theory,[31,32] the hole and electron mobility of NDIs and three thionated NDIs were calculated, and the relationship between the electronic properties and the structures of OSCs was investigated. The calculated electron mobility of P is higher than the experimental value, but it is in accordance with that of other *N*-substituted alkyl groups NDIs; this verifies that the model we used herein is reasonable.[8] The electron and hole mobility both increased with the increasing thionation number, and S3 even behaved as an ambipolar OSC. The electron mobility sequences were in accordance with the experimental results obtained at room temperature, in the order of P < *cis*-S2 < S3. *trans*-S2 has larger hole and electron mobility than *cis*-S2; this is consistent with the research on *cis–trans*-isomers.[33–36] The experimental and calculated results are different because the experiments have been conducted with thin films, whereas the calculations have been conducted based on crystal structures. It is generally accepted that single crystal transistors provide higher performances than thin film transistors of the same material. We hope that our investigation would provide support for the future design and fabrication of high-performance OSC materials.

2. Theory and computational methods

Based on the Einstein relation, the charge mobility in OSCs can be given as follows:

$$\mu = \frac{e}{k_B T} D \tag{1}$$

where the diffusion coefficient D is caused by hopping. If there is no correlation between charge hopping and the hopping motion is a homogeneous random walk,[37–39] the hopping rate can be written as follows:

$$D = \lim_{t\to\infty} \frac{1}{2n} \frac{\langle x(t^2)\rangle}{t} \approx \frac{1}{2n} \sum_i r_i^2 W_i P_i \tag{2}$$

where n is the spatial dimensionality, r_i is the center-of-mass distance between two neighboring molecules in the ith pathway, and P_i is the hopping probability, which can be calculated by: $P_i = W_i / \sum W_i$. W_i is the intermolecular hopping rate, which can be deduced by[31,32]

$$W = \frac{V^2}{\hbar}\left(\frac{\pi}{\lambda k_B T}\right)^{1/2} \exp\left(-\frac{\lambda}{4 k_B T}\right) \tag{3}$$

where V is the effective electronic coupling between neighboring molecules, λ is the reorganization energy, and T is the temperature. Eqn (3) will hold when V is significantly smaller than λ (at least half of λ).[24,40,41] From eqn (1)–(3), we can know that the hopping rate depends on two microscopic parameters: the effective electronic coupling V and the reorganization energy λ.

Recently, the effect of crystal thermal fluctuations on charge mobility has been taken into account while calculating some benchmark systems such as anthracene, pentacene, and rubrene.[41–43] Thermal fluctuations will increase the charge mobility and improve the precision, especially in the non-dominant transfer direction. Considering that not many studies have been reported on thionated NDIs and the electron mobility of P is far below that of other NDIs, X-ray crystal structures are used without further geometry optimization.[23] For the calculation of V, the GGA functionals and hybrid functionals have been widely used.[44–49] We adopted the site-energy corrected method and performed it with the PW91/TZ2P functional implemented in the Amsterdam density functional (ADF) program.[50,51] The PW91 functional is robust and the most widely used functional to calculate electronic couplings.[24,25,43] For comparison, we also used three other functionals (PBE,[52] PBE0,[53] and B3LYP[54]) to calculate the electronic couplings for the P dimer in four compounds. The reorganization energy λ consists of internal and external parts. Due to the low dielectric constants of molecular solids in organic crystals, the external reorganization energy could be neglected, and we only focused on the internal contribution.[55] The adiabatic potential energy surface method was adapted for the calculation of λ.[56]

$$\lambda_h = \lambda_0^+ + \lambda_+ = (E_0^* - E_0) + (E_+^* - E_+) \tag{4}$$

$$\lambda_e = \lambda_0^- + \lambda_- = (E_0^* - E_0) + (E_-^* - E_-) \tag{5}$$

An insightful interpretation for the meaning of the above-mentioned energy parameters is given in Fig. 1. For the full geometry optimizations of the monomer molecules, we used the B3LYP functional with the 6-311G(d,p) basis set performed with the Gaussian 09 package.[57–59] The hybrid functional B3LYP was mainly chosen to describe the properties, such as the energy of FMO, vertical ionization potential (VIP), adiabatic ionization potential (AIP), vertical electronic affinity (VEA), and adiabatic electron affinity (AEA), of the π-conjugated molecules.[24,41]

The orientation function establishes the quantitative relationship between angular resolution anisotropic mobility and

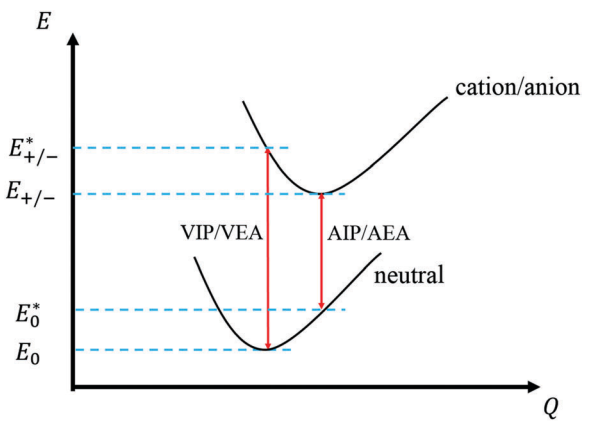

Fig. 1 Potential energy surfaces for the neutral state and the charged state.

molecular packing architecture parameters.[26,60] The function can be written as follows:

$$\mu_{\Phi} = \frac{e}{2k_{\mathrm{B}}T}\sum_{i} r_i^2 W_i P_i \cos^2\gamma_i(\theta_i - \Phi) \qquad (6)$$

where γ_i is the angle of the ith hopping pathway relative to the transport plane of the crystal stacking layer. For the hopping pathways on the basal transport stacking layer in the crystals, γ_i is 0°. θ_i is defined as the orientation angle of the projected electronic coupling pathways of different dimers, and Φ is the conducting channel relative to the same reference axis.

3. Results and discussion

As shown in Fig. 2, the monomers of the four crystals have similar structures, but a different number of O and S atoms. It is generally accepted that the vertical ionization potential (VIP) and vertical electron affinity (VEA) are related to material stability under ambient conditions and the injection efficiency of holes/electrons from the electrodes to the HOMOs/LUMOs.[61,62] As clearly presented in Table 1, the VIP and VEA decreased and increased, respectively; thus, the n- and p-type OSC properties improved with thionation degree. Upon comparing the VIP and VEA with the work function potential of a common gold electrode (E_g = 5.1 eV), it has been found that the VEA is closer to E_g than VIP for P, *cis*-S2, and *trans*-S2, whereas the VIP is even closer than the VEA for S3. This suggests that P, *cis*-S2, and *trans*-S2 are likely to behave as n-type OSCs, whereas S3 behaves as a p-type OSC.[63]

The energy levels of HOMOs and LUMOs are related to the electron affinity of organic materials.[24,28,61,64,65] Owing to the difference in the volume and polarization of O and S atoms, the frontier molecular orbitals (FMOs) of the four compounds show a remarkable change (Fig. 3). Upon the replacement of the O atoms by the S atoms, the distribution of LUMOs presents a larger difference than that for the HOMOs. Moreover, the energy of the HOMOs is higher and that for the LUMOs is lower. The decrease in the LUMO levels is favorable for higher electron carrier mobility as well as ambient stability.

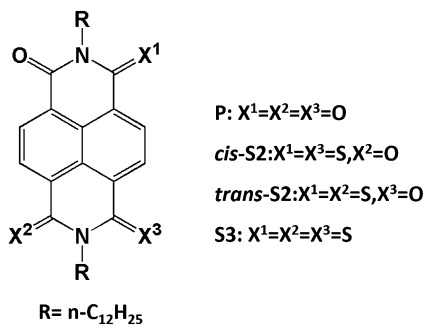

Fig. 2 Chemical structures of the four NDIs derivatives.

Table 1 Calculated VIP, AIP, VEA, and AEA (in eV) for the four compounds

	VIP	AIP	VEA	AEA
P	—	8.43	2.11	2.29
cis-S2	7.90	7.80	2.65	2.80
trans-S2	7.89	7.81	2.64	2.79
S3	7.78	7.72	2.88	3.01

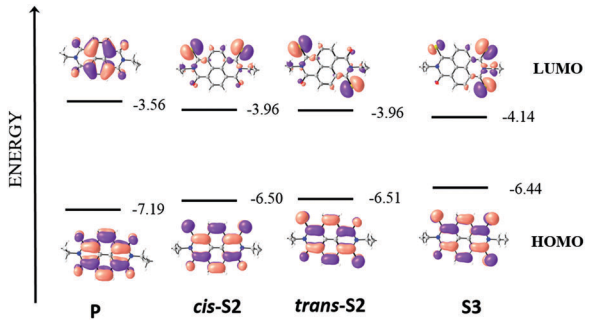

Fig. 3 The energy of HOMOs and LUMOs for the compounds P, *cis*-S2, *trans*-S2, and S3 at the B3LYP/6-311G(d,p) level (the alkane chains are neglected for clarity).

The calculated reorganization energy λ for the electron and hole transfer is listed in Table 2. As the number of S atoms increases, the reorganization energy of the holes and electrons (λ_h and λ_e, respectively) decreases. A high reorganization energy is not beneficial for high carrier transport; therefore, we have proposed that the charge mobility will increase with the increasing degree of thionation; this is consistent with the results obtained for electron mobility *via* experiments. Although the reorganization energy of holes is smaller than that for electrons, which implies that the four crystals are more likely to be p-type OSCs than to be n-type OSCs, the other factor of electronic coupling also affects the type of the four crystals. For compound P, we cannot calculate E_+^* since the energy is not converged. However, with the low value of E_{HOMO} and large VIP of P, we inferred that the compound P was unfavorable for hole carrier mobility.

Fig. 4a and b show the difference value of bond length (ΔL) between the charged and neutral states for *trans*-S2 and *cis*-S2, respectively. It can clearly be seen that ΔL between the anionic and neutral states (A–N) is larger than the value between the cationic and neutral states (C–N). For a deeper interpretation, we have calculated the average ΔL of all the bonds, which is 0.00775 Å (C–N for *trans*-S2), 0.00785 Å (C–N for *cis*-S2), 0.0163 Å (A–N for *trans*-S2), and 0.0168 Å (A–N for *cis*-S2). According to a previous study,[27] a conclusion can be drawn that the reorganization energy of electrons is higher than that of holes for *cis*-S2 and *trans*-S2, and the reorganization energy of *cis*-S2 is slightly higher than that of *trans*-S2 both for electrons and holes.

The intermolecular electronic coupling V is another important factor that influences charge mobility. For the four crystals, five types of intermolecular packing modes can be defined as

Table 2 Internal reorganization energies λ_h and λ_e (eV) for the four compounds

	P	*cis*-S2	*trans*-S2	S3
λ_h	—	0.197	0.177	0.122
λ_e	0.363	0.294	0.289	0.257

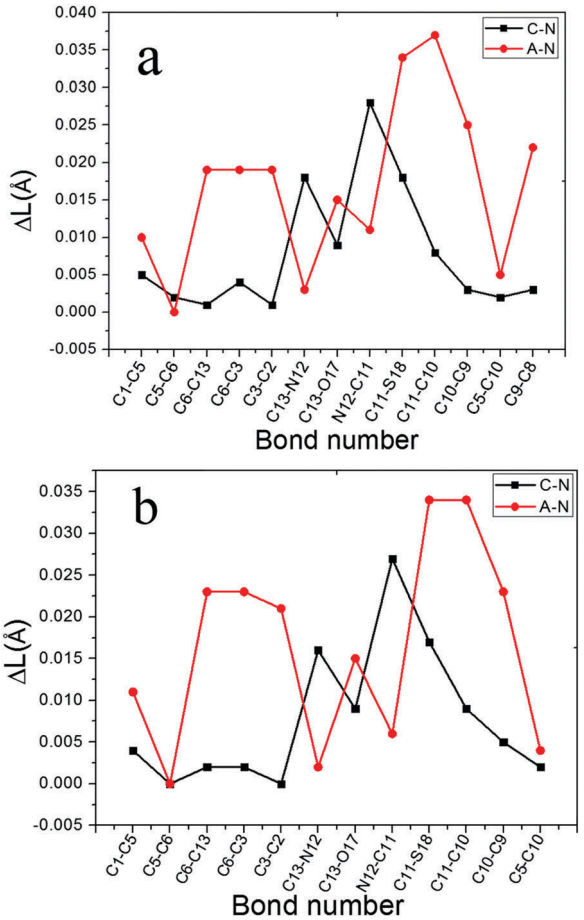

Fig. 4 Difference value of bond length (Δ*L*) between the cationic and neutral states (C–N labeled with black line) and between anionic and neutral states (A–N labeled with red line) in (a) *trans*-S2 and (b) *cis*-S2.

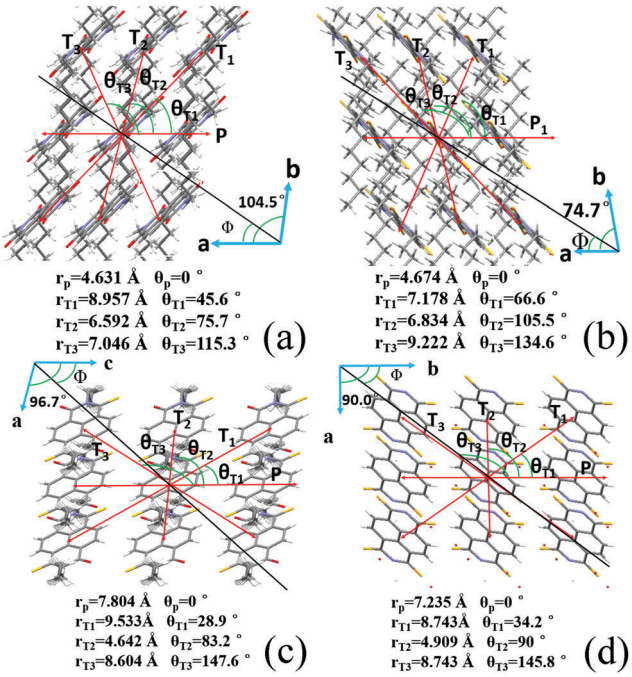

Fig. 5 Schematic of the molecular packing and charge hopping pathways in (a) P, (b) *cis*-S2, (c) *trans*-S2, and (d) S3 and the center-of-mass distance and angle of the projected electronic coupling pathways relative to the reference axis.

parallel dimer (P), transverse dimer (T1, T2, and T3), and longitudinal dimer (L). The P, T1, T2, and T3 dimers are in the same molecular stacking layers, as shown in Fig. 5. The L dimers are head-to-tail stacked outside the molecular stacking layer of the P, T1, T2, and T3 dimers. The calculated electronic coupling of the L dimer is very small, and the distances between the packing layers are larger than 28 Å; this means that charge transport between layers (L dimer) is less efficient and negligible; thus, charge transport in the four compounds can be considered as a 2D transport. The molecular packing of the four crystals is presented in Fig. 5, along with the hopping pathways and reference axis. For different dimers of each crystal, the center-of-mass distances corresponding to the hopping pathways of P, T1, T2, and T3 are labeled as r_P, r_{T1}, r_{T2}, and r_{T3}, and the angles are θ_P, θ_{T1}, θ_{T2}, and θ_{T3}, respectively (since the θ_P in each system is 0°, it is neglected herein). The orientation angle of the conducting channel relative to the reference axis is Φ.

The effective intermolecular electronic coupling V for the electron and hole transport of each packing mode in the four crystals is listed in Table 3. The values obtained with PW91 and PBE are almost equal, and the situation is same for the two hybrid functionals; thus, we only compare the difference between

Table 3 Calculated V_h and V_e for the different hopping pathways in the four compounds (the corresponding packing dimers are illustrated in Fig. 5)

	P		*cis*-S2		*trans*-S2		S3	
Pathway	V_h	V_e	V_h	V_e	V_h	V_e	V_h	V_e
P	1.8	32.6	0.76	21.3	12.7	57.5	9.3	124.4
P[a]	8.6	39.7	4.1	26.8	9.1	65.7	11.2	135.6
T1	2.1	30.4	0.10	0.85	7.8	12.0	0.05	0.18
T2	3.1	27.1	12.6	36.9	0.89	29.0	5.8	78.5
T3	0.03	0.47	4.5	35.3	0.18	2.1	49.3	36.1

[a] The electronic couplings for the P dimer in the four compounds were calculated with the B3LYP functional.

B3LYP and PW91. The values of V obtained with the GGA functionals are generally smaller than those for the hybrid functionals, especially for V_h, whereas V_e are close to each other, in which we are more interested. It can be found that all the maximum values of V_e are larger than the maximum values of V_h values in each crystal. These results suggest that the four compounds are n-type OSCs, which are contrary to the results of reorganization energy. Thus, by combining the effective electronic coupling with the reorganization energy results, we can obtain a reliable interpretation for the charge mobility. The maximum V_h values are in the sequence of P < *cis*-S2 ≈ *trans*-S2 < S3, whereas for V_e, the sequence is P < *cis*-S2 < *trans*-S2 < S3. Hence, we can conclude that the thionation effect will remarkably improve the charge transfer mobility for both electrons and holes.

Based on the crystals structures, effective electronic coupling, and reorganization energy, the anisotropic hole and electronic

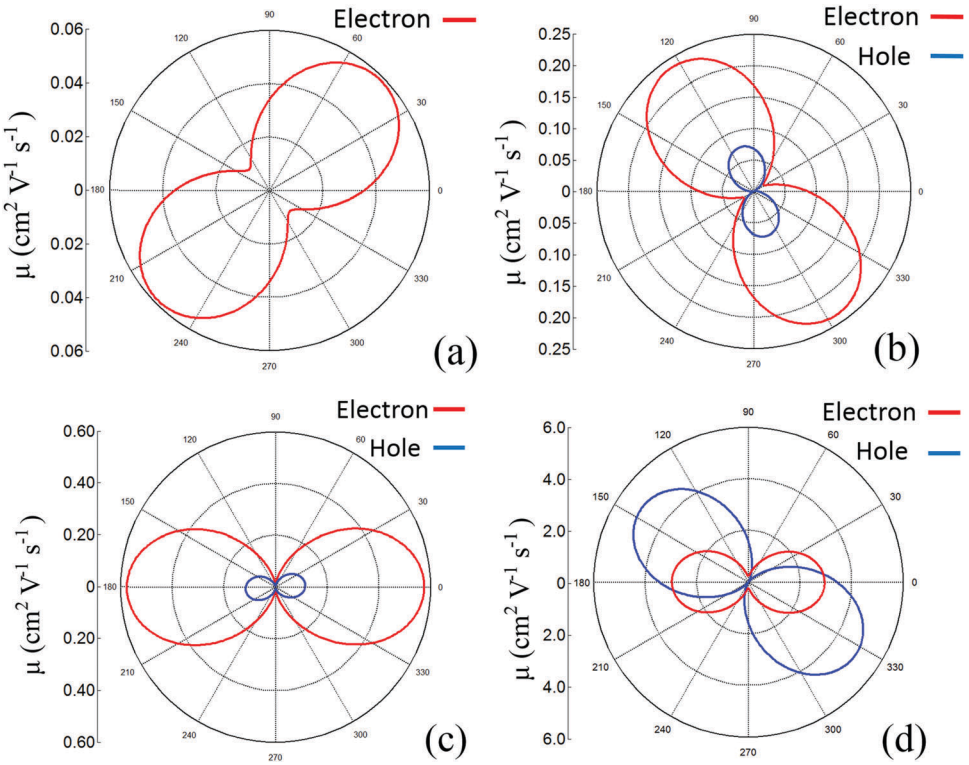

Fig. 6 Calculated angle-resolved anisotropic electron mobility (red line) and hole mobility (blue line) for the compounds (a) P, (b) *cis*-S2, (c) *trans*-S2, and (d) S3.

Table 4 The calculated hole and electron transport mobility (in $cm^2 V^{-1} s^{-1}$) and comparison with the experimental values

	$\mu_{h,cal}$	$\mu_{e,cal}$	$\mu_{e,exp}$
P	—	0.011–0.059	3.5×10^{-5} [a]
cis-S2	4.8×10^{-4}–0.074	0.019–0.24	0.022[a]
trans-S2	0.0043–0.12	0.013–0.58	—
S3	0.0017–5.02	0.22–2.96	0.047[a]

[a] The maximum electron mobility values at 30 °C.

mobility can be given *via* eqn (6) (Fig. 6, only the electron mobility is given for P). It can be found that the four crystals exhibit remarkable anisotropic carrier transfer and angular dependence on mobility. In Table 4, we have listed the calculated transport mobilities and compared them with the experimental values. It can be seen that the calculated result is higher than the experimental result. The main factor for this was that the theoretical calculations were based on the crystal structures, but the experiments were conducted with thin films. Other factors such as dielectric constant, deposition rate, and crystal defect will also reduce the mobility by several orders of magnitude.[15] Moreover, the development of fabrication techniques and gate dielectrics will enormously improve the performance of OSCs.[66] The model we used herein is reasonable because the calculated electron mobility of P matches well with that reported in other references, where the mobility of different *N*-substituted chain alkyl groups range from 10^{-3} to 0.1 $cm^2 V^{-1} s^{-1}$.[8]

For the compound P, the maximum value of electron mobility is 0.0587 $cm^2 V^{-1} s^{-1}$, which is at 45° with reference to the *a* axis. This direction is near the pathway of T1, where V_e is not largest. It is reasonable that the three electronic coupling values are almost in the direction of P, T1, and T2. The dominant orientations of electron and hole transfer are the direction of maximum effective electronic coupling in *cis*-S2 and in *trans*-S2. The two isomers show an n-type behavior, with *trans*-S2 giving a higher mobility for both holes and electrons. Generally, the carrier mobility of *trans*-isomers is higher than that of *cis*-isomers; this has been confirmed by a series of previous studies.[33–36] The carrier mobility of S3 is highest among the four structures, but it shows a p-type character. Unlike those of other structures, the favored directions of the hole and electron carrier mobility in S3 are different. The highest hole mobility value appears at $\Phi = 145°$, which is near the T3 dimer orientation. In contrast, for favorable electron mobility, Φ is close to 0° for the P dimer orientation.

From the calculated mobility anisotropy curve, we can summarize that (1) the hole and electron mobility increases with the increasing number of S atoms because P only behaves as a n-type organic semiconductor with a mobility value 0.0587 $cm^2 V^{-1} s^{-1}$, whereas S3 performs as an ambipolar OSC with its hole and electron mobility higher than 1.0 $cm^2 V^{-1} s^{-1}$ and (2) *trans*-S2 is more favorable for carrier mobility than *cis*-S2 for both holes and electrons.

4. Conclusions

In the present study, based on quantum-chemical calculations and the Marcus–Hush theory, the carrier mobility properties of

four naphthalene diimide and thionated naphthalene diimide crystals were calculated in detail. The results of FMO energy level, ionization potential, electron affinity, and reorganization energy indicate that thionation is beneficial for charge transfer of both electrons and holes. The compound P without thionation only behaves as an n-type OSC with a mobility value of 0.0587 $cm^2 V^{-1} s^{-1}$, whereas S3 behaves as an ambipolar OSC with both the hole and electron mobility higher than 3.0 $cm^2 V^{-1} s^{-1}$. With an increase in the number of S atoms, the compounds exhibit more p-type property: P, *cis*-S2, and *trans*-S2 behave as n-type OSCs, whereas S3 shows remarkable ambipolar type OSC behaviour. *trans*-S2 has a larger carrier hole and electron mobility than *cis*-S2; this is consistent with the previous results obtained for the *cis–trans* isomers. These results provide a guide for the optimization of OSC performance by analysis of the relationship between the carrier mobility property and molecular crystal structures. For a deeper systematic and comprehensive understanding of the thionation effect on the mobility properties of NDIs, three other structures should be synthesized and characterized in the future, which are mono-thionated, pre-thionated, and compounds with two S atoms in one diimide group.

Conflicts of interest

There are no conflicts to declare.

Acknowledgements

This work was supported by the National Natural Science Foundation of China (No. 21422309 and 21573229). G. J. Z. also thanks the Frontier Science Project of the Knowledge Innovation Program of Chinese Academy of Sciences (CAS), the Project for Excellent Member of CAS Youth Innovation Promotion Association, the Open Research Fund of State Key Laboratory of Bioelectronics, Southeast University, and the Double First-Rate Project of Tianjin University for the financial support.

References

1 F. C. Krebs, T. Tromholt and M. Jorgensen, *Nanoscale*, 2010, **2**, 873–886.
2 R. A. J. Janssen and J. Nelson, *Adv. Mater.*, 2013, **25**, 1847–1858.
3 G. Gelinck, P. Heremans, K. Nomoto and T. D. Anthopoulos, *Adv. Mater.*, 2010, **22**, 3778–3798.
4 J. G. Mei, Y. Diao, A. L. Appleton, L. Fang and Z. N. Bao, *J. Am. Chem. Soc.*, 2013, **135**, 6724–6746.
5 Y. G. Wen and Y. Q. Liu, *Adv. Mater.*, 2010, **22**, 1331–1345.
6 G. Heimel, I. Salzmann, S. Duhm and N. Koch, *Chem. Mater.*, 2011, **23**, 359–377.
7 I. Mcculloch, R. S. Ashraf, L. Biniek, H. Bronstein, C. Combe, J. E. Donaghey, D. I. James, C. B. Nielsen, B. C. Schroeder and W. M. Zhang, *Acc. Chem. Res.*, 2012, **45**, 714–722.
8 Y. Zhao, Y. Guo and Y. Liu, *Adv. Mater.*, 2013, **25**, 5372–5391.
9 H. Y. Li, B. C. K. Tee, J. J. Cha, Y. Cui, J. W. Chung, S. Y. Lee and Z. N. Bao, *J. Am. Chem. Soc.*, 2012, **134**, 2760–2765.
10 Y. B. Yuan, G. Giri, A. L. Ayzner, A. P. Zoombelt, S. C. B. Mannsfeld, J. H. Chen, D. Nordlund, M. F. Toney, J. S. Huang and Z. N. Bao, *Nat. Commun.*, 2014, **5**, 3005–3013.
11 J. Takeya, M. Yamagishi, Y. Tominari, R. Hirahara, Y. Nakazawa, T. Nishikawa, T. Kawase, T. Shimoda and S. Ogawa, *Appl. Phys. Lett.*, 2007, **90**, 102120.
12 K. Zhou, H. L. Dong, H. L. Zhang and W. P. Hu, *ChemPhysChem*, 2014, **16**, 22448–22457.
13 J. G. Laquindanum, H. E. Katz, A. Dodabalapur and A. J. Lovinger, *J. Am. Chem. Soc.*, 1996, **118**, 11331–11332.
14 G. Horowitz, F. Kouki, P. Spearman, D. Fichou, C. Nogues, X. Pan and F. Garnier, *Adv. Mater.*, 1996, **8**, 242.
15 D. Shukla, S. F. Nelson, D. C. Freeman, M. Rajeswaran, W. G. Ahearn, D. M. Meyer and J. T. Carey, *Chem. Mater.*, 2008, **20**, 7486–7491.
16 A. F. Lv, Y. Li, W. Yue, L. Jiang, H. L. Dong, G. Y. Zhao, Q. Meng, W. Jiang, Y. D. He, Z. B. Li, Z. H. Wang and W. P. Hu, *Chem. Commun.*, 2012, **48**, 5154–5156.
17 J. Sun, R. Devine, B. M. Dhar, B. J. Jung, K. C. See and H. E. Katz, *ACS Appl. Mater. Interfaces*, 2009, **1**, 1763–1769.
18 B. J. Jung, K. Lee, J. Sun, A. G. Andreou and H. E. Katz, *Adv. Funct. Mater.*, 2010, **20**, 2930–2944.
19 L. X. Tan, Y. L. Guo, Y. Yang, G. X. Zhang, D. Q. Zhang, G. Yu, W. Xu and Y. Q. Liu, *Chem. Sci.*, 2012, **3**, 2530–2541.
20 M. Nakano, K. Niimi, E. Miyazaki, I. Osaka and K. Takimiya, *J. Org. Chem.*, 2012, **77**, 8099–8111.
21 M. Nakano, H. Mori, S. Shinamura and K. Takimiya, *Chem. Mater.*, 2012, **24**, 190–198.
22 A. J. Tilley, C. Guo, M. B. Miltenburg, T. B. Schon, H. Yan, Y. N. Li and D. S. Seferos, *Adv. Funct. Mater.*, 2015, **25**, 3321–3329.
23 L. M. Kozycz, C. Guo, J. G. Manion, A. J. Tilley, A. J. Lough, Y. N. Li and D. S. Seferos, *J. Mater. Chem. C*, 2015, **3**, 11505–11515.
24 V. Coropceanu, J. Cornil, D. A. da Silva, Y. Olivier, R. Silbey and J. L. Bredas, *Chem. Rev.*, 2007, **107**, 926–952.
25 W. Q. Deng, L. Sun, J. D. Huang, S. Chai, S. H. Wen and K. L. Han, *Nat. Protoc.*, 2015, **10**, 632–642.
26 S. H. Wen, A. Li, J. L. Song, W. Q. Deng, K. L. Han and W. A. Goddard, *J. Phys. Chem. B*, 2009, **113**, 8813–8819.
27 S. H. Wen, W. Q. Deng and K. L. Han, *Phys. Chem. Chem. Phys.*, 2010, **12**, 9267–9275.
28 J. D. Huang, S. H. Wen and K. L. Han, *Chem. – Asian J.*, 2012, **7**, 1032–1040.
29 Y. Geng, S. X. Wu, H. B. Li, X. D. Tang, Y. Wu, Z. M. Su and Y. Liao, *J. Mater. Chem.*, 2011, **21**, 15558–15566.
30 S. P. Adiga and D. Shukla, *J. Phys. Chem. C*, 2010, **114**, 2751–2755.
31 R. A. Marcus, *J. Chem. Phys.*, 1956, **24**, 966–978.
32 N. S. Hush, *J. Chem. Phys.*, 1958, **28**, 962–972.
33 M. R. Rao, H. T. Black and D. F. Perepichka, *Org. Lett.*, 2015, **17**, 4224–4227.
34 M. Mamada, H. Katagiri, M. Mizukami, K. Honda, T. Minamiki, R. Teraoka, T. Uemura and S. Tokito, *ACS Appl. Mater. Interfaces*, 2013, **5**, 9670–9677.

35 M. Mamada, T. Minamiki, H. Katagiri and S. Tokito, *Org. Lett.*, 2012, **14**, 4062–4065.
36 D. Lehnherr, A. R. Waterloo, K. P. Goetz, M. M. Payne, F. Hampel, J. E. Anthony, O. D. Jurchescu and R. R. Tykwinski, *Org. Lett.*, 2012, **14**, 3660–3663.
37 C. L. Wang, F. H. Wang, X. D. Yang, Q. K. Li and Z. G. Shuai, *Org. Electron.*, 2008, **9**, 635–640.
38 W. Q. Deng and W. A. Goddard, *J. Phys. Chem. B*, 2004, **108**, 8614–8621.
39 E. Demiralp and W. A. Goddard, *Phys. Rev. B: Condens. Matter Mater. Phys.*, 1997, **56**, 11907–11919.
40 J. Cornil, J. L. Bredas, J. Zaumseil and H. Sirringhaus, *Adv. Mater.*, 2007, **19**, 1791–1799.
41 H. Yang, F. Gajdos and J. Blumberger, *J. Phys. Chem. C*, 2017, **121**, 7689–7696.
42 J. Arago and A. Troisi, *Adv. Funct. Mater.*, 2016, **26**, 2316–2325.
43 S.-F. Zhang, X.-K. Chen, J.-X. Fan and A.-M. Ren, *Org. Electron.*, 2013, **14**, 607–620.
44 K. Navamani and K. Senthilkumar, *RSC Adv.*, 2015, **5**, 38722–38732.
45 K. Navamani and K. Senthilkumar, *J. Phys. Chem. C*, 2014, **118**, 27754–27762.
46 A. Kubas, F. Gajdos, A. Heck, H. Oberhofer, M. Elstner and J. Blumberger, *Phys. Chem. Chem. Phys.*, 2015, **17**, 14342–14354.
47 A. Kubas, F. Hoffmann, A. Heck, H. Oberhofer, M. Elstner and J. Blumberger, *J. Chem. Phys.*, 2014, 140.
48 C. Schober, K. Reuter and H. Oberhofer, *J. Chem. Phys.*, 2016, 144.
49 F. Gajdos, S. Valner, F. Hoffmann, J. Spencer, M. Breuer, A. Kubas, M. Dupuis and J. Blumberger, *J. Chem. Theory Comput.*, 2014, **10**, 4653–4660.
50 E. F. Valeev, V. Coropceanu, D. A. da Silva, S. Salman and J. L. Bredas, *J. Am. Chem. Soc.*, 2006, **128**, 9882–9886.
51 G. te Velde, F. M. Bickelhaupt, E. J. Baerends, C. F. Guerra, S. J. A. Van Gisbergen, J. G. Snijders and T. Ziegler, *J. Comput. Chem.*, 2001, **22**, 931–967.
52 J. P. Perdew, K. Burke and M. Ernzerhof, *Phys. Rev. Lett.*, 1996, **77**, 3865–3868.
53 C. Adamo and V. Barone, *J. Chem. Phys.*, 1999, **110**, 6158–6170.
54 A. D. Becke, *J. Chem. Phys.*, 1993, **98**, 5648–5652.
55 J. E. Norton and J. L. Bredas, *J. Am. Chem. Soc.*, 2008, **130**, 12377–12384.
56 G. R. Hutchison, M. A. Ratner and T. J. Marks, *J. Am. Chem. Soc.*, 2005, **127**, 2339–2350.
57 M. J. Frisch, G. W. Trucks, H. B. Schlegel, G. E. Scuseria, M. A. Robb, J. R. Cheeseman, G. Scalmani, V. Barone, B. Mennucci, G. A. Petersson, H. Nakatsuji, M. Caricato, X. Li, H. P. Hratchian, A. F. Izmaylov, J. Bloino, G. Zheng, J. L. Sonnenberg, M. Hada, M. Ehara, K. Toyota, R. Fukuda, J. Hasegawa, M. Ishida, T. Nakajima, Y. Honda, O. Kitao, H. Nakai, T. Vreven, J. A. Montgomery, J. E. Peralta, F. Ogliaro, M. Bearpark, J. J. Heyd, E. Brothers, K. N. Kudin, V. N. Staroverov, R. Kobayashi, J. Normand, K. Raghavachari, A. Rendell, J. C. Burant, S. S. Iyengar, J. Tomasi, M. Cossi, N. Rega, J. M. Millam, M. Klene, J. E. Knox, J. B. Cross, V. Bakken, C. Adamo, J. Jaramillo, R. Gomperts, R. E. Stratmann, O. Yazyev, A. J. Austin, R. Cammi, C. Pomelli, J. W. Ochterski, R. L. Martin, K. Morokuma, V. G. Zakrzewski, G. A. Voth, P. Salvador, J. J. Dannenberg, S. Dapprich, A. D. Daniels, O. Farkas, J. B. Foresman, J. V. Ortiz, J. Cioslowski and D. J. Fox, *Gaussian 09, Revision C. 01*, Gaussian, Inc., Wallingford, CT, 2009.
58 R. Krishnan, J. S. Binkley, R. Seeger and J. A. Pople, *J. Chem. Phys.*, 1980, **72**, 650–654.
59 C. T. Lee, W. T. Yang and R. G. Parr, *Phys. Rev. B: Condens. Matter Mater. Phys.*, 1988, **37**, 785–789.
60 J. D. Huang, S. H. Wen, W. Q. Deng and K. L. Han, *J. Phys. Chem. B*, 2011, **115**, 2140–2147.
61 J. E. Anthony, A. Facchetti, M. Heeney, S. R. Marder and X. W. Zhan, *Adv. Mater.*, 2010, **22**, 3876–3892.
62 Y. Zhang, X. Cai, Y. Bian, X. Li and J. Jiang, *J. Phys. Chem. C*, 2008, **112**, 5148–5159.
63 C. R. Newman, C. D. Frisbie, D. A. da Silva, J. L. Bredas, P. C. Ewbank and K. R. Mann, *Chem. Mater.*, 2004, **16**, 4436–4451.
64 Y. Le, Y. Umemoto, M. Okabe, T. Kusunoki, K. I. Nakayama, Y. J. Pu, J. Kido, H. Tada and Y. Aso, *Org. Lett.*, 2008, **10**, 833–836.
65 Y. Ie, M. Nitani, M. Ishikawa, K. Nakayama, H. Tada, T. Kaneda and Y. Aso, *Org. Lett.*, 2007, **9**, 2115–2118.
66 C. Wang, H. Dong, W. Hu, Y. Liu and D. Zhu, *Chem. Rev.*, 2012, **112**, 2208–2267.